Electronic Supplementary Material (ESI) for ChemComm.


## Supporting Information

# Site-Recognition Boosted the Sensing Performance of Terbium based Organic Frameworks on $UO_2^{2+}$ Detection

Kexuan Li[a,#], Yuan-Jun Tong[b,#], Qian Liu[a], Shiyu Peng[b], Xinying Gong[b], Dongmei Wang[b], Zhengjun Gong[b,*]

[a] School of Chemistry, Southwest Jiaotong University, Chengdu, Sichuan 610031, China

[b] School of Environmental Science and Engineering, Southwest Jiaotong University, Chengdu 611756, Sichuan, China

[#] This author contributed equally to this work

* *Corresponding Authors, E-mail: gzj@swjtu.edu.cn (Z. Gong)*

## Table of contents

## Supplementary Experimental Section

**Materials and Reagents.** $Tb(NO_3)_3·6H_2O$, dimethylformamide (DMF), and 5,5′,5′′-(1,3,5-Triazine-2,4,6-triyltriimino)tris[1,3-benzenedicarboxylic acid] ($H_6$TDPAT) were purchased from Aladdin Reagent (Shanghai, China). $UO_2(NO_3)_2$ was purchased from Beijing HWRK Chem Co., Ltd (Beijing, China). All the other interfering compounds for $UO_2^{2+}$ detection experiments ( $BaCl_2·2H_2O$, $Mg(NO_3)_2·6H_2O$, $Al(NO_3)_3·9H_2O$, $Ca(NO_3)_2·4H_2O$, $Cd(NO_3)_2·4H_2O$, $Fe(NO_3)_3·9H_2O$, $Co(NO_3)_2·6H_2O$, $Zn(NO_3)_2·6H_2O$, $Na_2CO_3$, $NaHCO_3$, $NaNO_3$, $NaNO_2$, $Na_2SO_4$, $Na_2SO_3$, NaBr, and NaCl ) were purchased from Chengdu Kelong Chemical Reagent Factory. All suspensions were prepared using deionized water (resistivity > 18.2 MΩ cm).

**Apparatus.** The UV-vis spectra were collected on an UH4150 spectrophotometer (Hitachi, Japan). Quanta 200 scanning electron microscopy (SEM, U.S.A.) and JEOL2010 transmission electron microscope (TEM, Japan) were used to characterize the sizes and morphology. Fourier transform infrared (FT-IR) spectra was performed over a Specturm 2 spectrometer (PerkinElmer, USA) using KBr as reference. Fluorescence spectra were performed on an FLS1000 time-resolved fluorescence spectrometer. The excitation wavelength and slit widths (including excitation and emission) were set at 280 nm and 0.8 nm, respectively. The X-ray photoelectron spectroscopy (XPS) spectra were recorded on powders with a Thermo ESCALAB 250 spectrometer using an Al Ka monochromator source (hv=1486.6 eV) and a multi detection analyzer.

**Preparation of Tb-TDPAT.** Tb-TDPAT was synthesized as follows[1]: First, 0.1133 g of $Tb(NO_3)_3·6H_2O$ (0.25 mmol), 0.0773 g of $H_6$TDPAT (0.125 mmol) were dissolved in a mixed solution of 20 mL of DMA, and 10 mL of ethanol (EtOH). Finally, the solution was sealed in an autoclave and heated at 120 °C for 2 days. After cooling to room temperature, the final white powder was harvested via filtration from the organic phase, washed several times with water, ethanol, acetone in sequence, and dried in vacuum drying oven at 80 °C for 3h. The white powder product was named as Tb-TDPAT, Yield: 80% (based on $H_6$TDPAT).

**Experimental conditions optimization.** The effects of reaction time, temperature, and probe concentration were systematically studied at the $UO_2^{2+}$ concentration of 5 μM. At 25 ℃, the 100 μL of the obtained Tb-TDPAT stock suspension (0.2mg/mL) and the 200 μL of $UO_2^{2+}$ solution (15 μM) were mixed. The mixture was controlled to a final volume of 600 μL by ultrapure water. After the suspension was incubated for 1, 2, 5, 10, 20, 30, 40, 50 and 60 min, fluorescence spectra were

measured. As shown in Figure S6a, the fluorescence quenching efficiency $(F_0\text{-}F)/F_0$ increased and reached to plateau within five minutes. Furthermore, the reaction temperature was optimized under a 20 minutes reaction time (Figure S6b). Along with temperatures increased from 20 to 40 °C, the sensing performance of Tb-TDPAT on $UO_2^{2+}$ was rarely changed, demonstrating the probe could be worked in these temperatures. Therefore, subsequent experiments were conducted directly at room temperature. At room temperature, the 100 μL of the obtained Tb-TDPAT stock suspension (0.01, 0.05, 0.1, 0.2, 0.5, and 1 mg/mL) and the 200 μL of $UO_2^{2+}$ solution (15 μM) were mixed. The mixture was controlled to a final volume of 600 μL by ultrapure water. In Figure S7c, the quenching efficiency is stronger when the final concentration of probe is 16.67mg/L. The experimental results indicate that, the optimal detection conditions for $UO_2^{2+}$ by Tb-TDPAT was controlled at reaction time for 20 minutes, concentration of probe for 16.67 mg/L, reaction temperature for 25 °C.

**Examination of the probing performances to $UO_2^{2+}$.**The stock suspension of the Tb-TDPAT probe was produced by mixing the asprepared Tb-TDPAT (5 mg) to ultrapure water (50 mL) under continuous sonication for 3 min. Then, the 100 μL of the obtained Tb-TDPAT stock suspension and an aliquot of $UO_2^{2+}$ solution (200 μL) were mixed. The mixture was controlled to a final volume of 600 μL by ultrapure water. After the suspension was incubated for 20 min, fluorescence spectra was measured. A stock solution of $UO_2^{2+}$ (1000 μM) was prepared by dissolving a precisely weighed amount of uranyl nitrate hexhydrate ($UO_2(NO_3)_2{\cdot}6H_2O$) in ultrapure water. Working standard solutions were prepared by diluting the stock solution suitably with deionized water to give various concentrations of $UO_2^{2+}$ from 100 μM to 0.01 μM. The fluorescence peak of $Tb^{3+}$ at 545 nm was used for quantification. In order to eliminate the error induced by the suspension change or instrument fluctuation, all spectra were collected in parallel for three times, and the average data were used for plotting.

**Selectivity of the assay to $UO_2^{2+}$.** To evaluate the sensing selectivity of the Tb-TDPAT system for $UO_2^{2+}$, potential interfering ions in complexed environment were used to investigate the anti-interfering capacity of Tb-TDPAT. Metal ions ($UO_2^{2+}$, $Mg^{2+}$, $Al^{3+}$, $Zn^{2+}$, $Fe^{3+}$, $Cd^{2+}$, $Co^{2+}$, $Ca^{2+}$, $Ba^{2+}$) and anions ($SO_3^{2-}$, $NO_3^-$, $NO_2^-$, $HCO_3^-$, $CO_3^{2-}$, $Cl^-$, $Br^-$, $SO_4^{2-}$) were dissolved in ultrapure water. 100 μL nanoprobe suspension (100 mg $L^{-1}$), 300 μL ions solution and 200 μL ultrapure water were to control the total volume of 600 μL. The concentration of $UO_2^{2+}$ was set at 2 μM, the concentrations

of metal ions were 5 folds of $UO_2^{2+}$, and the concentrations of anions were 10 or 25 folds of $UO_2^{2+}$. Finally, the resulting mixtures were allowed to stand by for 20 min and then were used for fluorescent measurements under the same conditions. All experiments were performed in triplicate and the error bars in the figures are the standard deviation of the three parallel experiments.

**Analysis of $UO_2^{2+}$ in real water samples.** To test the general applicability of Tb-TDPAT probe, standard addition method was performed on the water samples (the Wahaha mineral water) for our assay. Subsequently, 60 μL of the mineral water samples, 200μL $UO_2^{2+}$ solution and 100 μL of Tb-TDPAT probe(0.1mg/mL) were diluted to 700 μL with ultrapure water. The concentrations of $UO_2^{2+}$ in the tested water samples are presented in Table S1.

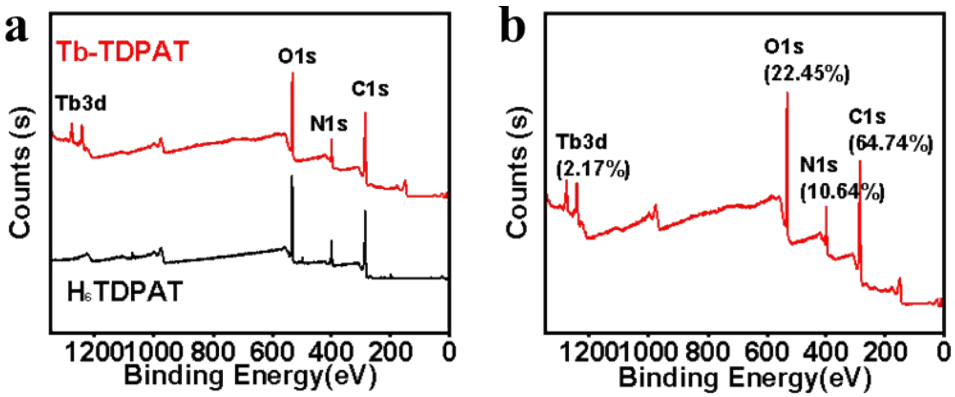


**Figure S1.** (a) XPS spectra of $H_6$TDPAT and Tb-TDPAT, respectively. (b) The contents of element in Tb-TDPAT.

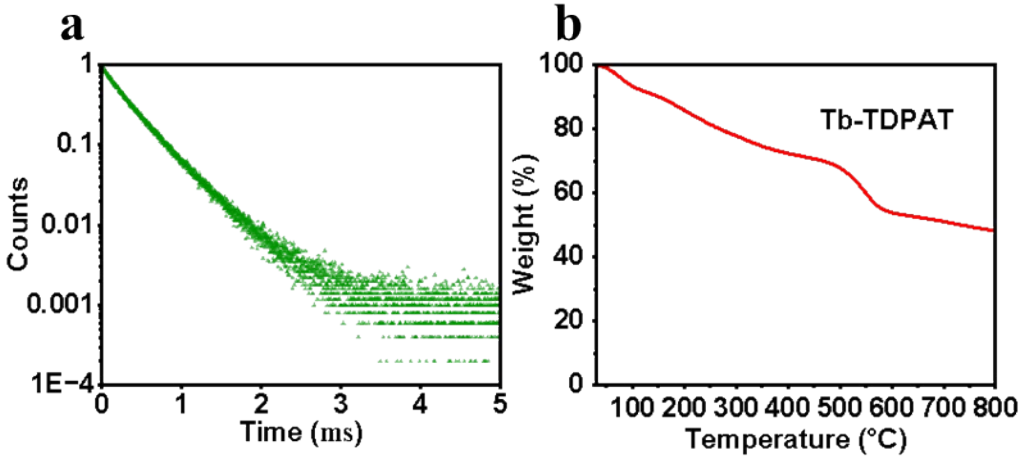


**Figure S2** (a) Fluorescence decay curves of Tb-TDPAT. (b) TGA curve of Tb-TDPAT under $N_2$ atmosphere.

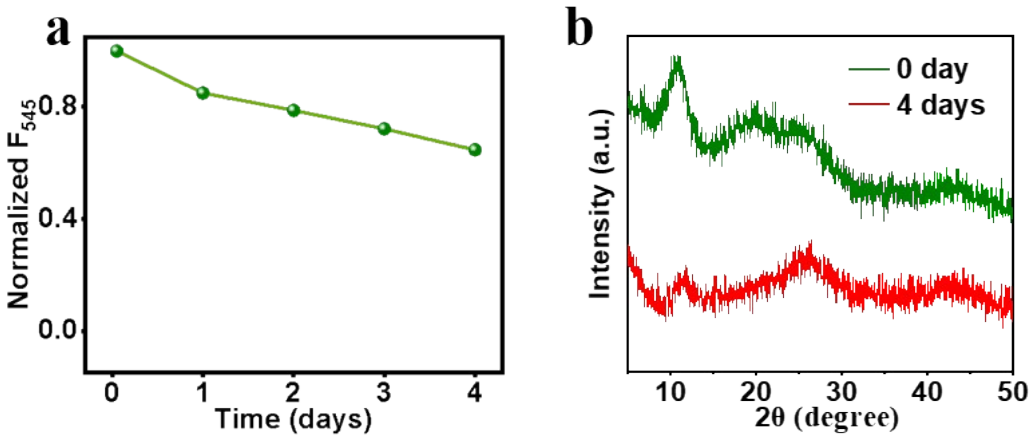


**Figure S3.** (a) The fluorescence emission intensity of Tb-TDPAT under the water treatment. (b) The PXRD pattern of Tb-TDPAT before and after soaking in water for 4 days.

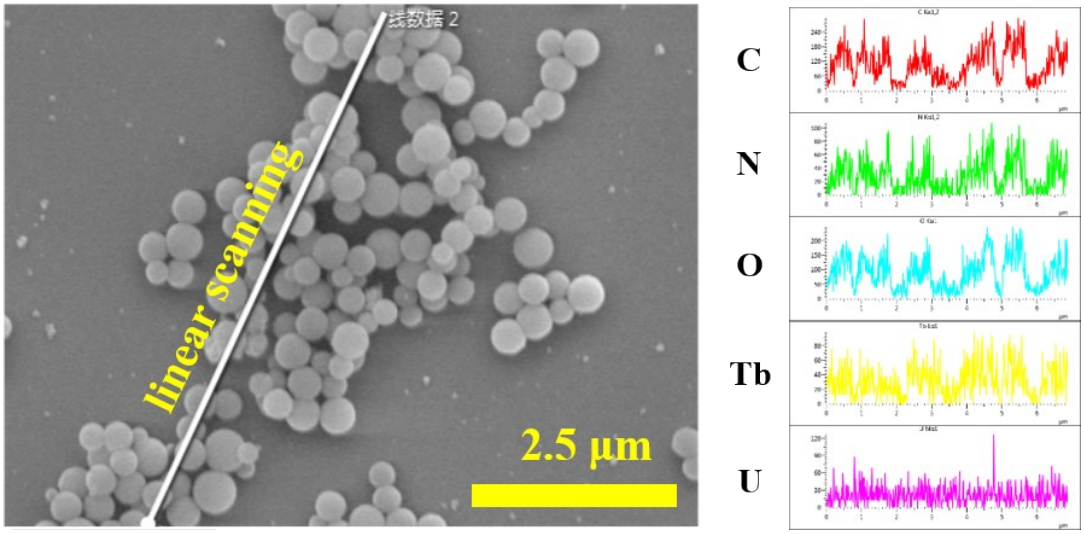


**Figure S4.** Scanning electron microscopic (SEM) image and energy dispersive spectrometry (EDS) of Tb-TDPAT, respectively.

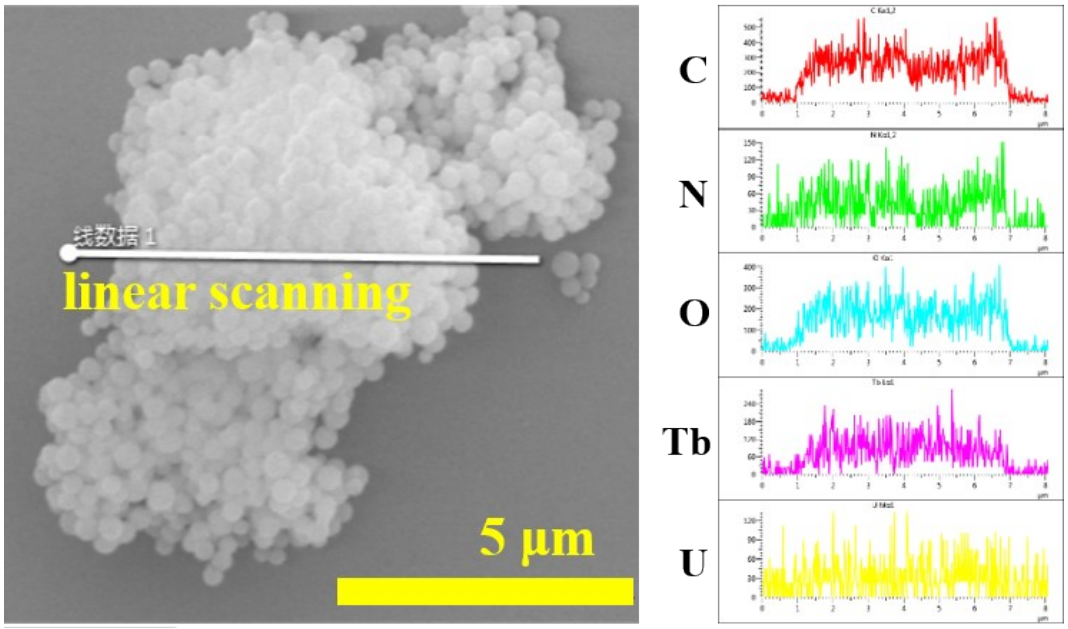


**Figure S5.** Scanning electron microscopic (SEM) image and energy dispersive spectrometry (EDS) of Tb-TDPAT in the presence of $UO_2^{2+}$, respectively.

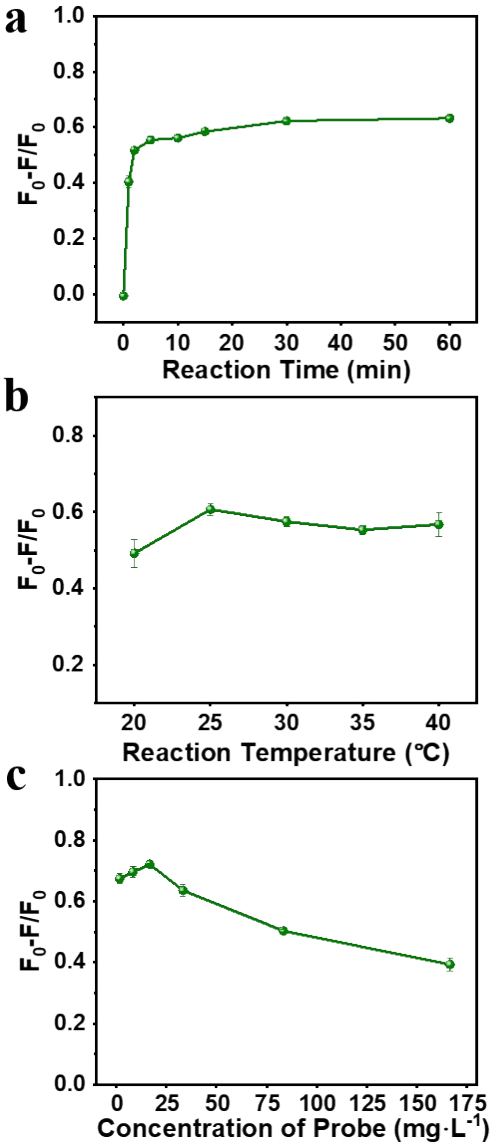


**Figure S6.** (a) The fluorescence quenching efficiency under different reaction time. (b) The fluorescence quenching efficiency under different reaction temperature. (c) The fluorescence quenching efficiency under different concentration of probe.

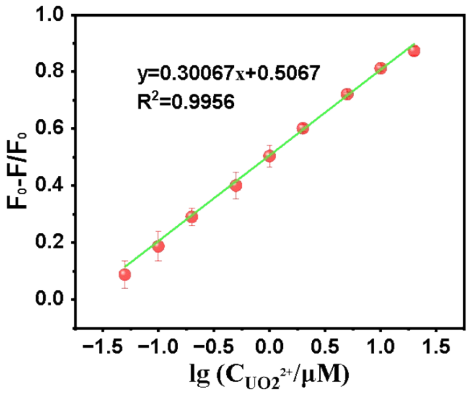


**Figure S7.** Linear regression curve ranging from 0.05 to 20 μM.

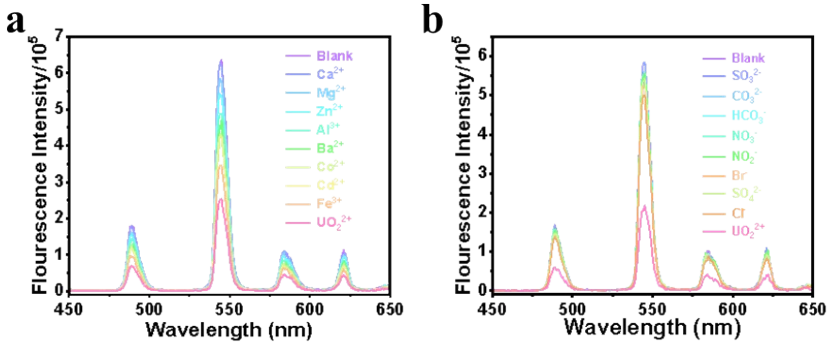


**Figure S8.** The fluorescence spectra of the Tb-TDPAT upon addition of different ions (a) 2 μM: $UO_2^{2+}$. 10 μM: $Mg^{2+}$, $Al^{3+}$, $Zn^{2+}$, $Fe^{3+}$, $Cd^{2+}$, $Co^{2+}$, $Ca^{2+}$, $Ba^{2+}$. (b) 2 μM: $UO_2^{2+}$. 20 μM: $SO_3^{2-}$, $NO_3^-$, $NO_2^-$, $HCO_3^-$, $CO_3^{2-}$. 50 μM: $Cl^-$, $Br^-$, $SO_4^{2-}$.

**Table S1.** Various fluorescent sensing strategies for detection of $UO_2^{2+}$.

| Method | Response mode | Materials | Linear range (nM) | LOD (nM) | References |
|---|---|---|---|---|---|
| Fluorescence | turn-off | ZIF-90 | 1083-13000 | 3.9 | 2 |
| Fluorescence | turn-on | DNAzyme | 866-4333333 | 0.43 | 3 |
| Fluorescence | turn-off | Organic fluorophore | 40-450 | 4.7 | 4 |
| Fluorescence | turn-on | DNAzyme | 0-500 | 0.19 | 5 |
| Fluorescence | turn-off | Ln-MOFs | 0-13000 | 3.9 | 6 |
| Fluorescence | turn-off | Ln-MOFs | 50-20000 | 1.25 | This work |

**Table S2.** Actual analysis of $UO_2^{2+}$ in mineral water samples.

| Samples | Added (μM) | Founded (μM) | Recovery (%)[a] | RSD (%, =3) |
|---|---|---|---|---|
| Mineral water | 0 | 0.02±0.00 | N.A. | N.A. |
| | 0.5 | 0.45±0.04 | 86.0 | 7 |
| | 1 | 1.07±0.15 | 105.0 | 15 |
| | 5 | 5.34±0.26 | 106.4 | 5 |
| | 10 | 9.52±0.66 | 95.0 | 7 |
| Fu River | 0 | 0.02±0.00 | N.A. | N.A. |
| | 5 | 5.21±0.23 | 103.8 | 9 |
| | 10 | 10.66±0.17 | 106.4 | 2 |
| | 15 | 14.23±0.90 | 94.7 | 6 |

**N.A.: not available**

**Recovery=($C_{Founded}$-$C_0$)/$C_{Added}$**

## References


1 H. S. Li, S. Yu, Q. L. Guan, Z.-X. You, F.-Y. Bai, S. Jiang and Y.-H. Xing, *Cryst. Growth Des.*, 2023, **23**, 6557-6569.

2 D. Mei and B. Yan, *J. Hazard. Mater.*, 2023, **447**, 130822.

3 W. Yun, H. Wu, X. Liu, H. Zhong, M. Fu, L. Yang and Y. Huang, *Sensors and Actuators B: Chemical*, 2018, **255**, 1920-1926.

4 H. Ding, C. Li, H. Zhang, N. Lin, W.-S. Ren, S. Li, W. Liu, Z. Xiong, B. Xia and C.-C. Wang, *Chin. Chem. Lett.*, 2023, **34**, 107725.

5 M. Feng, C. Gu, Y. Sun, S. Zhang, A. Tong and Y. Xiang, *Anal. Chem.*, 2019, **91**, 6608-6615.

6 W. Liu, X. Dai, Z. Bai, Y. Wang, Z. Yang, L. Zhang, L. Xu, L. Chen, Y. Li, D. Gui, J. Diwu, J. Wang, R. Zhou, Z. Chai and S. Wang, *Environ. Sci. Technol.*, 2017, **51**, 3911-3921.